Mass Cytometry: Technique for Real Time Single Cell Multitarget Immunoassay Based on Inductively Coupled Plasma Time-of-Flight Mass Spectrometry

ARTICLE *in* ANALYTICAL CHEMISTRY · JULY 2009

Impact Factor: 5.64 · DOI: 10.1021/ac901049w · Source: PubMed

10 AUTHORS, INCLUDING:

Dmitry R Bandura

Fluidigm Corporation

32 PUBLICATIONS **1,742** CITATIONS

SEE PROFILE

Olga Ornatsky

Fluidigm Canada, Inc.

64 PUBLICATIONS **3,250** CITATIONS

SEE PROFILE

Xudong Lou

Fluidigm Canada, Inc.

31 PUBLICATIONS **1,549** CITATIONS

SEE PROFILE

Anal. Chem. **2009,** *81,* 6813–6822

Mass Cytometry: Technique for Real Time Single Cell Multitarget Immunoassay Based on Inductively Coupled Plasma Time-of-Flight Mass Spectrometry

Dmitry R. Bandura,*,† Vladimir I. Baranov,† Olga I. Ornatsky,† Alexei Antonov,‡ Robert Kinach,† Xudong Lou,† Serguei Pavlov,‡ Sergey Vorobiev,‡ John E. Dick,§ and Scott D. Tanner†,‡

Department of Chemistry, University of Toronto, 80 St. George Street, Toronto, Ontario M5S 3H6, Canada, DVS Sciences, Inc., 70 Peninsula Crescent, Richmond Hill, Ontario L4S 1Z5, Canada, and University Health Network, Toronto Medical Discovery Tower, 101 College Street, Toronto, Ontario M5G 1L7, Canada

A novel instrument for real time analysis of individual biological cells or other microparticles is described. The instrument is based on inductively coupled plasma time-of-flight mass spectrometry and comprises a three-aperture plasma−vacuum interface, a dc quadrupole turning optics for decoupling ions from neutral components, an rf quadrupole ion guide discriminating against low-mass dominant plasma ions, a point-to-parallel focusing dc quadrupole doublet, an orthogonal acceleration reflectron analyzer, a discrete dynode fast ion detector, and an 8-bit 1 GHz digitizer. A high spectrum generation frequency of 76.8 kHz provides capability for collecting multiple spectra from each particle-induced transient ion cloud, typically of 200−300 μs duration. It is shown that the transients can be resolved and characterized individually at a peak frequency of 1100 particles per second. Design considerations and optimization data are presented. The figures of merit of the instrument are measured under standard inductively coupled plasma (ICP) operating conditions (<3% cerium oxide ratio). At mass resolution (full width at half-maximum) $M/\Delta M > 900$ for $m/z = 159$, the sensitivity with a standard sample introduction system of $>1.4 \times 10^8$ ion counts per second per mg L^{-1} of Tb and an abundance sensitivity of $(6 \times 10^{-4})-(1.4 \times 10^{-3})$ (trailing and leading masses, respectively) are shown. The mass range ($m/z = 125-215$) and abundance sensitivity are sufficient for elemental immunoassay with up to 60 distinct available elemental tags. When <15 elemental tags are used, a higher sensitivity mode at lower resolution ($M/\Delta M > 500$) can be used, which provides $>2.4 \times 10^8$ cps per mg L^{-1} of Tb, at $(1.5 \times 10^{-3})-(5.0 \times 10^{-3})$ abundance sensitivity. The real-time simultaneous detection of multiple isotopes from individual 1.8 μm polystyrene beads labeled with lanthanides is shown. A real time single cell 20 antigen expression assay of model cell lines and leukemia patient samples immuno-labeled with lanthanide-tagged antibodies is presented.

The unambiguous functional and phenotypical identification of cells in heterogeneous populations requires quantitative determination of many biomarkers simultaneously in individual cells.[1] A similar requirement for multiparameter assays is shared by genomic and proteomic researchers interested in understanding the complex interaction of many genes, proteins, and small molecules which lead to the transformation of a normal cell into a disease causing cell. Currently available flow cytometry technologies based on fluorescence are generally limited to 10 simultaneous measurements. Recently, 17-plex polychromatic flow cytometry data from stimulated peripheral blood mononuclear cells was demonstrated.[2] The main limitations of the existing flow cytometers are related to the spectral overlap between signals from fluorescent labels used in analysis,[3] be it organic dyes or quantum dots, the latter having a narrower emission bandwidth (~30 nm full width at half-maximum, ~70 nm at 10% of maximum[4]).

We have developed a new approach for the detection of proteins and other molecules in individual cells. The approach is based on attaching specially designed multiatom elemental tags to antibodies, in place of fluorescent labels, and takes advantage of the high resolution, sensitivity, and speed of analysis of inductively coupled plasma time-of-flight mass spectrometry (ICP-TOF-MS). Since many available stable isotopes can be used in the tags, many proteins and gene transcripts can potentially be detected simultaneously in individual cells through the quantification of stable isotope tags bound to target biomarkers.

Nomizu et al.[5] demonstrated the vaporization, atomization, and ionization of individual cells by inductively coupled plasma and

* Corresponding author. Phone: +1 416 946 8420. Fax: +1 416 978 4317. E-mail: Dmitry.Bandura@utoronto.ca.

† University of Toronto.

‡ DVS Sciences, Inc.

§ University Health Network.

(1) Roederer, M.; DeRosa, S.; Gerstein, R.; Anderson, M.; Bigos, M.; Stovel, R.; Nozaki, T.; Parks, D.; Herzenberg, L.; Herzenberg, L. *Cytometry* **1997**, *29*, 328–339.

(2) Perfetto, S. P.; Chattopadhyay, P. K.; Roederer, M. *Nat. Rev. Immunol.* **2004**, *4*, 648–655.

(3) Roederer, M. *Cytometry* **2001**, *45*, 194–205.

(4) Bruchez, M., Jr.; Moronne, M.; Gin, P.; Weiss, S.; Alivisatos, A. P. *Science* **1998**, *281* (5385), 2013–2016.

(5) Nomizu, T.; Kaneco, S.; Tanaka, T.; Ito, D.; Kawaguchi, H.; Vallee, B. T. *Anal. Chem.* **1994**, *66*, 3000–3004.

10.1021/ac901049w CCC: $40.75
Published on Web 07/14/2009

used an optical emission ICP spectrometer to detect endogenous calcium in individual air-borne dried cells. The same group later employed ICPMS for the detection of individual air-borne zinc particles.[6] Recently, Tanner et al. reported the acquisition of single element transient ion signals by quadrupole ICPMS from individual air-borne cells stained with gold-labeled antibodies or rhodium-DNA intercalator.[7] The method of simultaneous detection by ICPMS of multiple proteins in homogeneous biological samples using element-tagged antibodies, first suggested and demonstrated by Baranov et al.[8−10] and further developed by several groups,[11−16] cannot be directly applied to multitarget individual cell analysis. First, the quadrupole mass analyzers, used to date, have settling time of ~50−200 μs, which is required for stabilization of the mass filter between individual isotope measurements. This time is longer than the duration of the ion cloud produced in ICP from an individual microparticle (~100 μs fwhm[17]). Thus, measurement of two or more isotopes during a transient event of such short duration is virtually impossible with scanning analyzers. This points to the need for a simultaneous mass analyzer, such as a time-of-flight analyzer or a magnetic sector analyzer with an array detector. Existing ICP-TOF mass spectrometers generate single scan full mass spectra at frequencies as high as 33 000 spectra/s, which would almost satisfy the need for individual cell analysis, if not for the fact that these instruments only display and record processed, integrated spectra at a maximum spectra recording rate of 50−78 spectra/s.[18,19] The required frequency of sampling and recording of the cell-induced transient has to be much higher, e.g., 50 000−100 000 spectra/s, to allow for 10 or more individual spectra per particle, so that the transients from overlapping particles can be recognized.

Second, the number of metal atoms per tag in commercially available antibody tagging probes (for example, AutoDelfia reagents from PerkinElmer Life and Analytical Sciences, Shelton, CT) is 6−10, which in consideration of the dynamic range of interest for biomarker detection (10^2−10^6 copies of a biomarker per cell), places a requirement for the combined efficiency of sample utilization to be at least 1 ion detected per 1000 atoms of a tag. The existing ICP-TOF-MS instruments have an ion transmission efficiency of approximately 1 ion detected for each 5×10^5 ions produced in the plasma (estimate for $m/z = 100$ at 10^7 counts per second per mg/L sensitivity). The required improvement in detection power can be achieved by either increasing the number of atoms per tag (described in ref 20), improvement of the transmission efficiency of the mass spectrometer, or more likely, both.

Recently, our group published preliminary results of a feasibility study for detection of multiple isotopes from short cell- and bead-induced transient ion clouds produced in the ICP via TOF-MS format.[21] The ICP-TOF-MS research "breadboard" instrument, described briefly in ref 21, was built around the vacuum system and a modified TOF section of a commercial ESI-TOF-MS. It operated at 55 000 spectra/s frequency, acquired data with significant data loss (50% or more, depending on the number of measured isotopes), had a limited dynamic range detector (based on microchannel plates), detected ~1 ion for each 5×10^4 ions produced in the plasma, and had relatively low (~1%) cell introduction efficiency.

This article describes the detailed design considerations and analytical characteristics of the new, purpose-designed prototype mass cytometer,[22] with specific attention to real-time, no data loss, higher sensitivity, higher spectral frequency, higher dynamic range single cell elemental immuno-analysis. We also show its first application to a 20-antigen expression assay of model cell lines and leukemia patient samples.

EXPERIMENTAL SECTION

Materials. Instrument tuning solutions were prepared by sequential dilution in 0.1% HNO_3 [Baseline, Seastar Chemicals Inc., Sidney, BC, Canada] in deionized water (Gradient, Millipore, Bedford, MA) of the all-lanthanide standard (PE Pure Plus Multielement Calibration Standard 2, PerkinElmer Instruments, Shelton, CT) or single-element standards (Spex CertiPrep, Metuchen, NJ). For single particle analysis tuning, 1.8 μm diameter amine-modified polystyrene microspheres (PA04N/7603, Bangs Laboratories, Inc., Fishers, IN) were further modified by conjugation to diethylene triamine pentaacetic acid (DTPA), washed several times, and resuspended in 100 μL of carbonate buffer (pH 9.6) at 7.5×10^8 particles/mL. Tb, Ho, and Tm lanthanide solutions at 5 mg/L were prepared in 0.1% HNO_3 from the 1000 mg/L stock solutions, then diluted to 0.5 mg/L with incubation buffer comprising 10 mM NH_4OAc, 0.5 mM NaOH (pH 5.5) (also used as a wash buffer). A volume of 10 μL of the DTPA-beads suspension were added to 1 mL of incubation buffer, then 0.5 mL added to 0.5 mL of the 0.5 mg/L total Tb + Ho + Tm concentration in a ratio of 1:2:1, and incubated overnight at room temperature. The solutions were then transferred to 100K molecular weight cutoff (MWCO) spin filters and washed with 0.5 mL of wash buffer five times at 3000*g* for 2 min. The particles were then resuspended in 2 mL

(6) Kaneco, S.; Nomizu, T.; Tanaka, T.; Mizutani, N.; Kawaguchi, H. *Anal. Sci.* **1995**, *11*, 835–840.
(7) Tanner, S. D.; Ornatsky, O.; Bandura, D. R.; Baranov, V. I. *Spectrochim. Acta, Part B* **2007**, *62*, 188–195.
(8) Baranov, V.; Tanner, S.; Bandura, D.; Quinn, Z. *Elemental Analysis of Tagged Biologically Active Materials*. U.S. Patent 7,135,296, November 14, 2006.
(9) Baranov, V. I.; Bandura, D. R.; Tanner, S. D. ICP-MS As an Elemental Detector in Immunoassays. Speciation without Chromatography. In *European Winter Conference on Plasma Spectrochemistry*, Book of Abstracts, Lillehammer, Norway, February 4−8, 2001; p 85.
(10) Baranov, V. I.; Quinn, Z.; Bandura, D. R.; Tanner, S. D. *Anal. Chem.* **2002**, *74*, 1629–1636.
(11) Zhang, C.; Wu, F.; Zhang, Y.; Wang, X.; Zhang, X. *J. Anal. At. Spectrom.* **2001**, *16*, 1393–1396.
(12) Zhang, C.; Zhang, Z. Y.; Yu, B. B.; Shi, J. J.; Zhang, X. R. *Anal. Chem.* **2002**, *74*, 96–99.
(13) Zhang, S. C.; Zhang, C.; Xing, Z.; Zhang, X. R. *Clin. Chem.* **2004**, *50*, 1214–1221.
(14) Hutchinson, R. W.; Ma, R. L.; McLeod, C. W.; Milford-Ward, A.; Lee, D. *Can. J. Anal. Sci. Spectrosc.* **2004**, *49*, 429–435.
(15) Ornatsky, O. I.; Baranov, V. I.; Bandura, D. R.; Tanner, S. D.; Dick, J. *J. Immunol. Methods* **2006**, *308*, 68–76.
(16) Careri, M.; Elviri, L.; Maffini, M.; Mangia, A.; Mucchino, C.; Terenghi, M. *Rapid Commun. Mass Spectrom.* **2008**, *22*, 807–811.
(17) Stewart, I. I.; Olesik, J. W. *J. Am. Soc. Mass Spectrom.* **1999**, *10*, 159–174.
(18) Myers, D. P.; Hieftje, G. M. *Microchem. J.* **1993**, *48*, 259–277.
(19) Moore, L.; Bandura, D. *The Advantages of Time-of-Flight Mass Spectrometry for Elemental Analysis.*; GBC Scientific Equipment ICPMS Technical Note, GBC Scientific Equipment: Melbourne, Australia, 1998.
(20) Lou, X.; Zhang, G.; Herrera, I.; Kinach, R.; Ornatsky, O.; Baranov, V.; Nitz, M.; Winnik, M. A. *Angew. Chem., Int. Ed.* **2007**, *46*, 6111–6114.
(21) Tanner, S. D.; Bandura, D. R.; Ornatsky, O.; Baranov, V. I.; Nitz, M.; Winnik, M. A. *Pure Appl. Chem.* **2008**, *80*, 2627–2641.
(22) Now commercially available as the CyTOF, DVS Sciences Inc., Richmond Hill, Ontario, Canada.

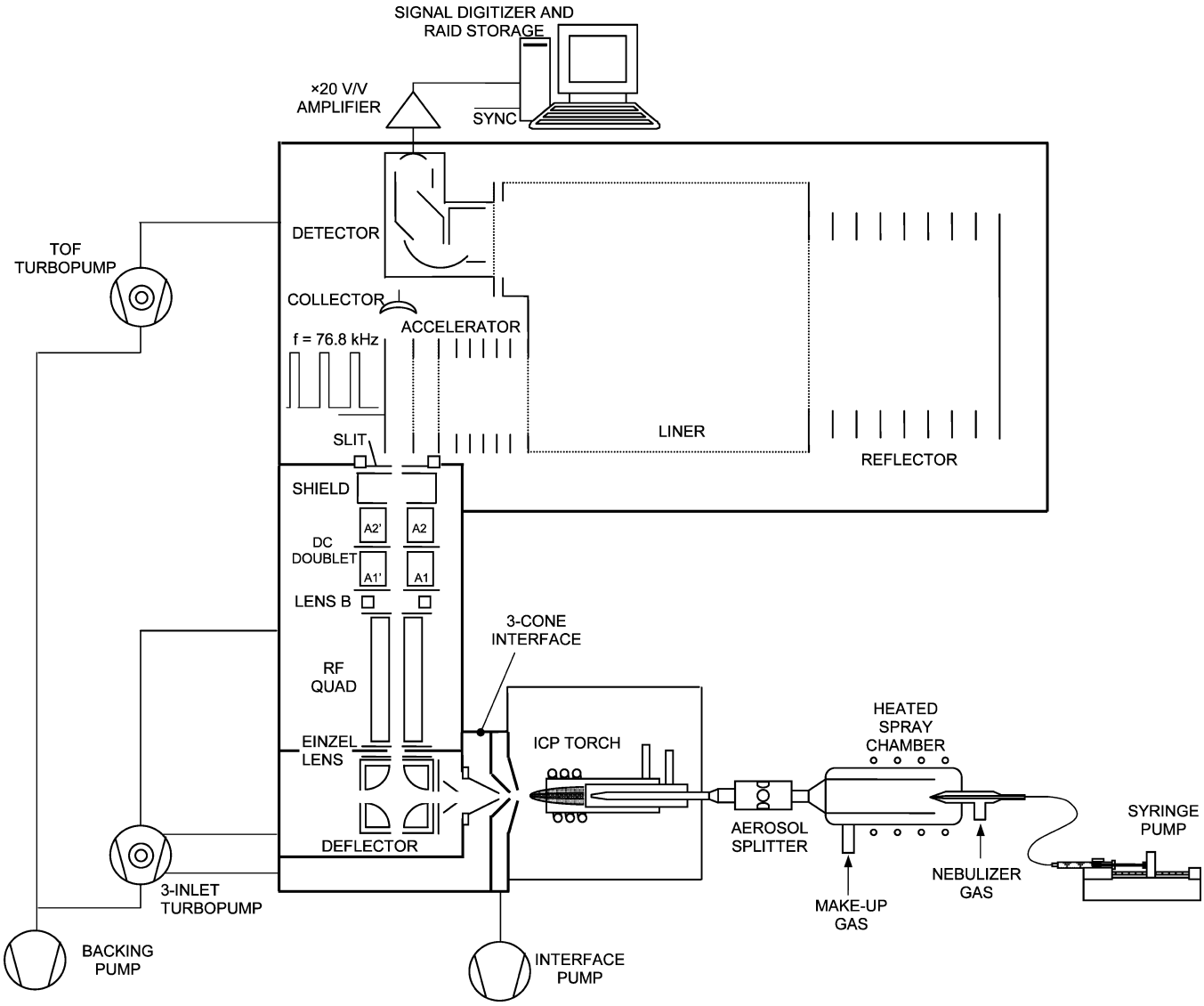

Figure 1. Schematics of the prototype CyTOF mass cytometer.

of wash buffer, with $\sim 2 \times 10^6$ beads per mL final concentration. The suspensions were shaken/vortexed right before analysis. The preparation of the cell samples is described in the cell analysis section.

Instrument Description. The schematic of the new instrument is shown in Figure 1. Cells or other particles are introduced in the form of a liquid suspension by the syringe pump (Pump 22, Harvard Apparatus Canada, Saint-Laurent, Québec, Canada) and aspirated by a concentric nebulizer (TQ-30-A1, Meinhard Glass Products, Golden, CO). For cell analysis, the nebulizer is connected to a custom-made heated spray chamber, to which a makeup Ar gas flow (typically at 5 L/min) is supplied via a mass flow controller. This high flow of heated makeup gas is needed to partially dry the larger droplets that contain cells and to provide adequate confinement of the high inertia larger droplets in the gas stream. An aerosol splitter is positioned between the spray chamber and the ICP torch. The splitter allows a fraction of the particle-containing gas stream (typically 0.9 L/min out of ~6 L/min) into the torch injector. For instrument tuning and $\sim 1\ \mu$m beads analysis, a cyclonic spray chamber (PN 300-19MS, Precision Glassblowing, Centennial, CO), which allows only a small-diameter fraction of aerosol through, can be used with either a peristaltic pump (Minipuls 3, Gilson, Inc., Middleton, WI) or the syringe pump. For this prototype instrument, the plasma generator is adapted from the ELAN 6000 ICPMS (Perkin-Elmer-SCIEX, Concord, ON, Canada) and comprises a free-running (nominal 40 MHz) radiofrequency generator and an rf-balanced load coil arrangement. The torch assembly is also from the ELAN and comprises a demountable torch and a 2 mm i.d. quartz injector.

The plasma is sampled through an interface which has 3 apertures: sampler (1.1 mm orifice diameter), skimmer (1 mm diameter), and reducer (1.2 mm diameter). The sampler−skimmer region is pumped by a 40 m^3/h rotary pump (Sogevac 40, Oerlikon Leybold Vacuum, Köln, Germany) and the skimmer−reducer region by the Holweck stage of a three-stage cartridge turbo-molecular pump (TW400/300/25, Oerlikon Leybold Vacuum). The intermediate stage of the three-stage pump evacuates the portion of the vacuum chamber containing the ion deflection optics, and the high vacuum stage pumps the region containing the ion beam shaping optics. The TOF section is evacuated with a separate turbo-molecular pump (TW250S, Oerlikon Leybold Vacuum). Typical pressures in the five stages of the vacuum system with the ICP operating under standard conditions ($CeO^+/Ce^+ \leq 3\%$) are P1 = 2.3 Torr, P2

= 28 mTorr, P3= 350 μTorr, P4 = 3 μTorr, and P5 = 0.3 μTorr, respectively.

The core of the supersonic plasma jet propagates through the reducer orifice, ions are accelerated and focused by an electrostatic field defined by the potentials of the reducer and a conical lens and then are deflected by the electrostatic quadrupole deflector,[23,24] while unionized particles from the jet exit the deflector on a straight path to the turbo-molecular pump. Ion deflection is activated only when data acquisition is requested so that the total exposure of the ion optics and the detector to the ion beam is reduced. An einzel lens downstream of the deflector, consisting of the deflector exit aperture, ion guide entrance aperture, and an aperture between them, focuses the deflected ions into the rf-only quadrupole ion guide. An electrostatic quadrupole doublet downstream of the ion guide shapes the ion beam exiting the round exit aperture of the ion guide into a beam of cross-section compatible with the rectangular entrance slit (3 mm × 12 mm) of the orthogonal-acceleration reflectron time-of-flight analyzer. The low mass cutoff of the quadrupole ion guide is set close to $m/z = 80$, so that the low mass dominant plasma ions (O^+, OH^+, O_2^+, Ar^+, ArH^+, ArO^+) are unstable in the rf field and are ejected. The axial kinetic energy of the ions during transmission through the ion guide is kept at ~150 eV, which mitigates space-charge related ion loss in the ion guide. For the selected length of the field (127 mm) and the frequency of the rf drive (819.2 kHz), the lightest dominant ions (C^+ for biological samples) traverse the field in ~2 rf cycles, which is sufficient for their rejection.

The analyzer is operated at 76.8 kHz spectra generation frequency. A fast TOF ion detector (model 14882, ETP Electron Multipliers, SGE International Pty. Ltd., Ringwood, Victoria, Australia) is used for ion detection. The output signal of the detector is amplified by a preamplifier (FTA420, ORTEC Products Group, Oak Ridge, TN) and digitized by the analog-to-digital conversion (ADC) based 8-bit 1 GHz signal digitizer (PDA1000, Signatec, Inc., Newport Beach, CA). A trigger delay (9000 ns) and the recording segment length (3072 ns) are set to allow digitization of the segment of the signal that corresponds to m/z = 125−215, with 1 ns sampling resolution. The data stream and the instrument parameters are controlled by specially developed software.[22] Two distinct modes of instrument control are realized: instrument tuning mode and raw data collection mode. Instrument tuning is done with online integration of user-selected analytical mass channels and for which the results (typically integrated ion counts per 0.5 s reading) are displayed in real-time and can be saved as text files. The software routines allow automated optimization of all ion optics potentials and detector optimization. In this tuning mode, each 0.5 s integration requires 0.5−1.5 s (depending on the number of analytes selected for tuning) for data processing and storage, e.g., data loss of >50% is encountered. The raw data collection mode provides for no data loss, which is necessary for particle or cell analysis. Data digitized at 1 GHz from the PDA1000 are continuously recorded with no loss by the RAID system at a rate of 250 MB/s. This no-loss continuous experiment recording has been verified for up to 30 min. The maximum length of the recording is limited by the available space on the RAID system. In a typical cell analysis experiment, 2 min of raw data (~28 GB) is recorded as a single continuous record, containing all 9 216 000 single spectral segments (3072 ns long each) generated during the 2 min.

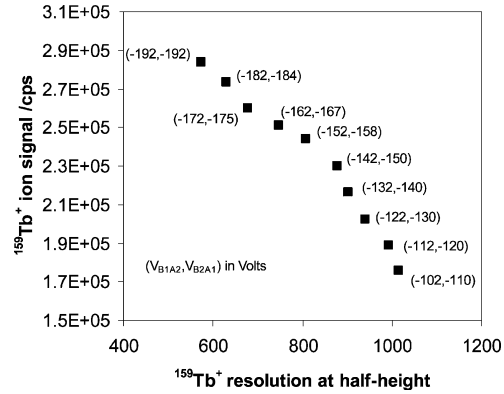

Figure 2. Ion signal for 1 ng/mL Tb sample and resolution for the $^{159}Tb^+$ peak at half height at different optima of the doublet pole pairs potentials measured at constant shield (−160 V) and doublet apertures (−80 V) potentials.

The time-of-flight analyzer is a single stage mass-reflectron[25] with two-stage[26] orthogonal acceleration.[27] The orthogonal acceleration TOF technology is widely used and has been well described (see, for example, refs 28−30). One significant difference of our analyzer is the use of a rather high (−120 V) bias of the orthogonal accelerator, which keeps ions at a relatively high kinetic energy, mitigating potential deterioration of resolution for transient events of extreme ion density. The biggest effect on the resolution of orthogonal acceleration TOF-MS is that of the near-emitter chromatic aberration in the first acceleration gap,[31] which scales as $(\Delta E_{i\perp}/E_0)^{1/2}$, where $\Delta E_{i\perp}$ is the ion energy spread in the time-of-flight direction, and E_0 is the field strength in the acceleration gap.[32] The energy spread $\Delta E_{i\perp}$ is defined by the quality of the point-to-parallel beam transfer by the doublet. The doublet consists of two sets of four rods, entrance, exit, and intermediate apertures, and a field-free region at the exit, screened by the shield. Two rods of the first set (shown as A1, A1′ in Figure 1) are electrically connected together and to the rod pair (B2, B2′, not shown) of the second set and biased to a potential V_{A1B2}. Similarly, rods of the first set (B1, B1′, not shown) are connected together and to the rods A2, A2′ of the second set and biased to a potential V_{A2B1}. Figure 2 shows results of the optimization of the doublet potentials and its effect on the instrument mass resolution.

(23) Zeman, H. D. *Rev. Sci. Instrum.* **1977**, *48*, 1079–1085.
(24) Mahaffy, P. R.; Lai, K. *J. Vac. Sci. Technol., A: Vac. Surfaces Films* **1990**, *8*, 3244–3246.
(25) Karataev, V. I.; Mamyrin, B. A.; Schmikk, D. V. *J. Tech. Phys.* **1971**, *16*, 1498–1505. Mamyrin, B. A.; Karataev, V. I.; Shmikk, D. V.; Zagulin, V. A. *Sov. Phys.-J. Exp. Theor. Phys.* **1973**, *37*, 45–52.
(26) Wiley, W. C.; McLaren, I. H. *Rev. Sci. Instrum.* **1955**, *26*, 1150–1157.
(27) O'Halloran, G. J.; Fluegge, R. A.; Betts, J. F.; Everett, W. J. Report No. ASD-TDR-62-644, Part 1 and 2: Determination of Chemical Species Prevalent in a Plasma Jet. Technical Report prepared by the Bendix Corporation Research Laboratories Division, Southfield, Michigan, under Contract Numbers AF33(616)-8374 and AF33(657)-11018. A.F. Materials Laboratory Research and Technology Division, Air Force Systems Command, 1964.
(28) Chernushevich, I. V.; Ens, W.; Standing, K. G. *Anal. Chem.* **1999**, *71*, 452A–461A.
(29) Guilhaus, M.; Selby, D.; Mlynski, V. *Mass Spectrom. Rev.* **2000**, *19*, 65–107.
(30) Ray, S. J.; Hieftje, G. M. *J. Anal. At. Spectrom.* **2001**, *16*, 1206–1216.
(31) Zavoisky, E. K.; Fanchenko, S. D. *Dokl. Akad. Nauk SSSR* **1956**, *108*, 218–221.
(32) Bandura, D. R.; Makarov, A. A. *Int. J. Mass Spectrom. Ion Processes* **1993**, *127*, 45–55.

Table 1. Figures of Merit for the Two Modes of Operation

parameter	value in high-resolution mode	value in high-sensitivity mode
dc quadrupole doublet		
doublet apertures	−80 V	−80 V
poles A1B2 potential	−110 V	−210 V
poles A2B1 potential	−102 V	−210 V
shield	−160 V	−120 V
sensitivity for continuous aspiration at <3% oxide ratio/cps per ppb		
$^{139}La^+$	>60 000	>100 000
Tb^+	>140 000	>240 000
Tm^+	>130 000	>220 000
$^{193}Ir^+$	>35 000	>60 000
$m/z = 181.5$ (background)/cps	<10	<30
resolution at half height ($m/z = 159$)	>900	>500
abundance sensitivity		
158/159 (peak areas)	$<1.4 \times 10^{-3}$	$<5 \times 10^{-3}$
160/159 (peak areas)	$<6 \times 10^{-4}$	$<1.5 \times 10^{-3}$

Two modes of operation can be utilized for cell analysis by a relatively simple change of instrument parameters. When the number of the antigens of interest is sufficiently large as to require resolution of adjacent (at $\Delta m/z = 1$) mass channels at better than 0.1% peak height, "high-resolution" mode at $M/\Delta M \cong 900-1000$ can be used. When the number of antigens of interest is lower, isotopes for tagging the antibodies can be selected at least two m/z channels apart, and "high-sensitivity" mode can be utilized. Table 1 summarizes the parameters of the instrument and typical figures of merit for the two modes.

The typical duration of the transient cell-induced ion cloud is 200−300 μs;[7] hence, the instrument background (per particle) is less than 10^{-2} counts and is thus negligible. A typical mass spectrum for $m/z = 136-176$ for the integral of 40 000 spectra (0.52 s acquisition time) for a sample of all (natural abundance) lanthanides at 20 pg/mL is shown in Figure 3.

Ion Detection, Signal Handling, and Data Processing. The dynamic range of ion detection is limited by the linearity range of the detector, dynamic range of the preamplifier−digitizer combination, instrument background, and acquisition time. In a conventional ICP-TOF MS, with time-to-digital conversion (TDC) utilized for ion counting, the dead time of the TDC defines the upper limit of the ion counting range. For 10 s acquisition at 30 kHz, assuming that the pulse "pile up" at 5 ns dead time is insignificant at <0.2 ions/event, a dynamic range of more than 4 orders of magnitude is available. In the present instrument, operated at 76.8 kHz spectra generation frequency, a single cell-induced transient event is characterized by approximately 25 sequential spectra. For events of such length, the ion counting only mode provides a dynamic range of about an order of magnitude. We use ADC data from the PDA1000 digitizer to provide both the pseudoion counting mode for low-intensity signals and analog mode detection for higher signals. In the pseudocounting mode, distinct peaks from single ions within each m/z time-of-flight interval are detected separately in each single spectrum. A simple peak detection algorithm, based on comparison of each sampling point within the given time-of-flight interval

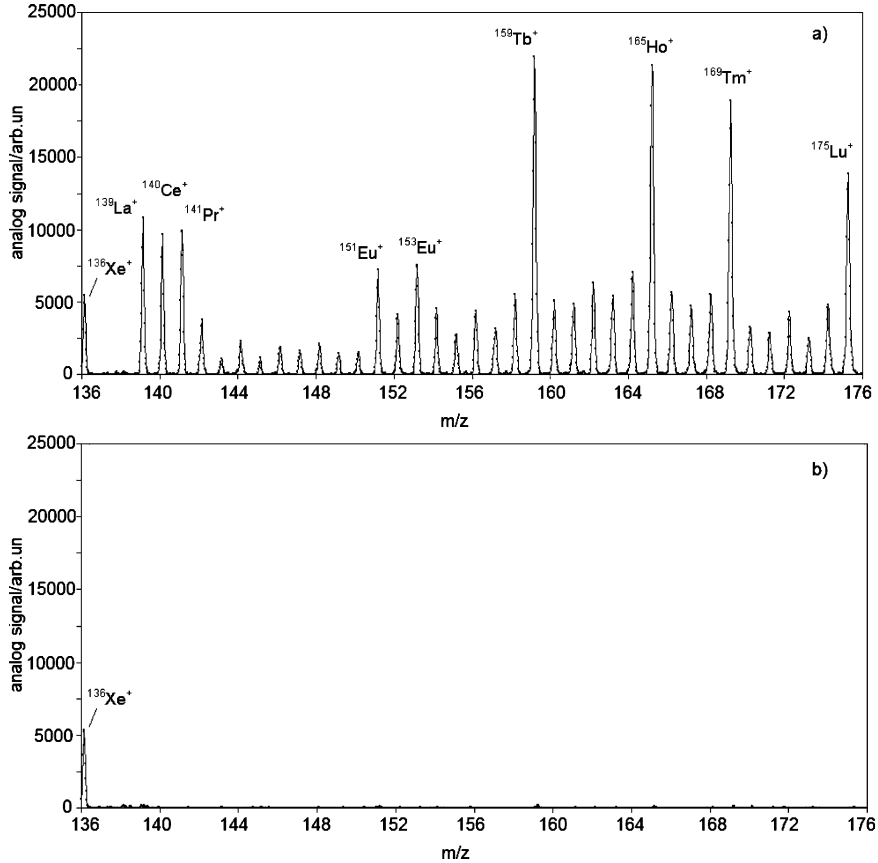

Figure 3. $m/z = 136-176$ segment of integral of 40 000 single mass spectra (0.52 s acquisition time) for a sample of all (natural abundance) lanthanides at 20 pg/mL each (a) and the blank (b) collected in high-resolution mode.

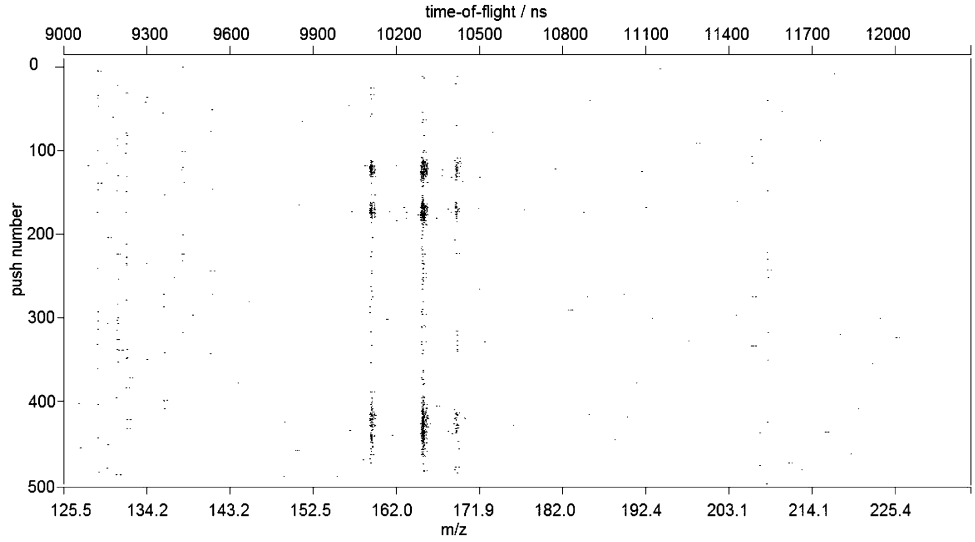

Figure 4. Screenshot of 500 consecutive spectra (total of 6.5 ms) for a sample of beads containing Tb, Ho, and Tm at 1:2:1 concentration.

to two adjacent sampling points, is used. Cross-calibration between the modes is done in the tuning mode with pseudocounting and analog data collected at various efficiencies of the optics for the detector cross-calibration solution achieved by varying the repelling poles potential. The data are analyzed for the best linear fit correlation between the analog and pseudocounting signals on running 10 consecutive points in the range 0−50 000 cps for each analyte, and the slopes and intercepts for analog-to-pulse conversion are derived to obtain the "dual mode" data. Five orders of magnitude linear dynamic range is available at 1 s integration. For single transient events of 25 spectra duration, a range of at least 1−1000 ions per event should be feasible, with opportunity for extension to higher signals by lowering the detector gain or increasing the PDA board voltage range.

In addition to the "external" dual mode calibration described above, the dual mode coefficients can be determined from raw particles/cells sample analysis data. In this case, the data is sorted to bins according to the selected intervals of analog signals, and the average pulse response for each analog intensity is calculated. The user then selects the pulse counting range (in pulses per spectrum), and the analog-to-pulse conversion coefficients are derived from the range data.

For a quick preview of the data before recording continuous raw data, a continuously refreshed screen display of 500 consecutive spectra is used (Figure 4). The horizontal scale represents the time-of-flight segment between 9 000−12 072 ns collected for each consecutive spectrum, and the vertical scale is the spectrum (push) number. The lower horizontal scale is the m/z scale derived from the known mass calibration. The data presentation is binary: the presence of an ion signal above a threshold at a particular TOF in a particular spectrum is represented as a point. The instrument background is ∼10 counts/s per mass channel or about 0.07 counts per mass channel summed over the 500 spectra shown in Figure 4.

Three transient events representing metal-encoded beads are shown in the figure, with short streaks of 10−30 spectra length at m/z = 159, 165, and 169. There is almost continuous background signal between the short streaks at the same masses, which is attributed to free metal in the buffer. The signals in the lower mass range are from isotopes of Xe impurity in the Ar. The width of the streaks is ∼15−20 points (ns) and represents the width of the mass peaks at their base. For cell/particle analysis, the first stage of processing of the raw data record comprises integration of user-selected mass channels within each single spectrum, compressing the data by a factor of $3072/2N$, where N is the number of selected mass channels (2 Bytes of data for each). When 30 mass channels are selected, the resulting compression factor is ∼50. The resulting files (typically <1 GB) contain "per spectrum" analog, pseudopulse, and dual data for the selected masses. Raw data for the beads shown in Figure 4 were collected for 120 s in high-resolution mode, and the data for each spectrum for m/z = 159, 165, and 169 were integrated within 16 ns-long integration windows, starting from ∼3% peak height. The resultant per-mass data for each of the first 64 000 consecutive spectra are shown in Figure 5.

The per-spectrum data were further processed in order to identify individual particle- or cell-induced transients (as opposed to discontinuous signal from the metals in solution). The algorithm for particle-induced transient detection includes adding all dual count signals for m/z = 159, 165, and 169 together in each spectrum, then smoothing the summed data using a Gaussian kernel of the $\sigma = 3$ spectra width. Thresholding of the smoothed data at $n = 5$ counts per spectrum flags "positive" events and is used to determine the width of each transient ("cell length"). Then, unsmoothed data for each m/z is integrated for each transient within its "cell length", producing a table with the transient start address (starting spectrum number), the length, and the integral for each m/z. The data is saved in text and in FCS3.0 formats, the latter being compatible with flow cytometry data processing software, for example, FlowJo.[33] For the example given in Figure 5, using $\sigma = 3$ and threshold of 5 counts per spectrum, 12 463 events were recorded in a 120 s measurement (9.2 million consecutive spectra record), of which 9 192 events had cell lengths of 12 or more consecutive spectra (e.g., >150 μs) and can be classified as particle-induced. The mean of the cell length was 21 spectra (270 μs). The cell length distribution of all 12 463 events, the resulting 2-D 10% contour plots, and their histograms for the bead events are shown in Figure 6.

(33) FlowJo Software, TreeStar Inc., http://www.flowjo.com.

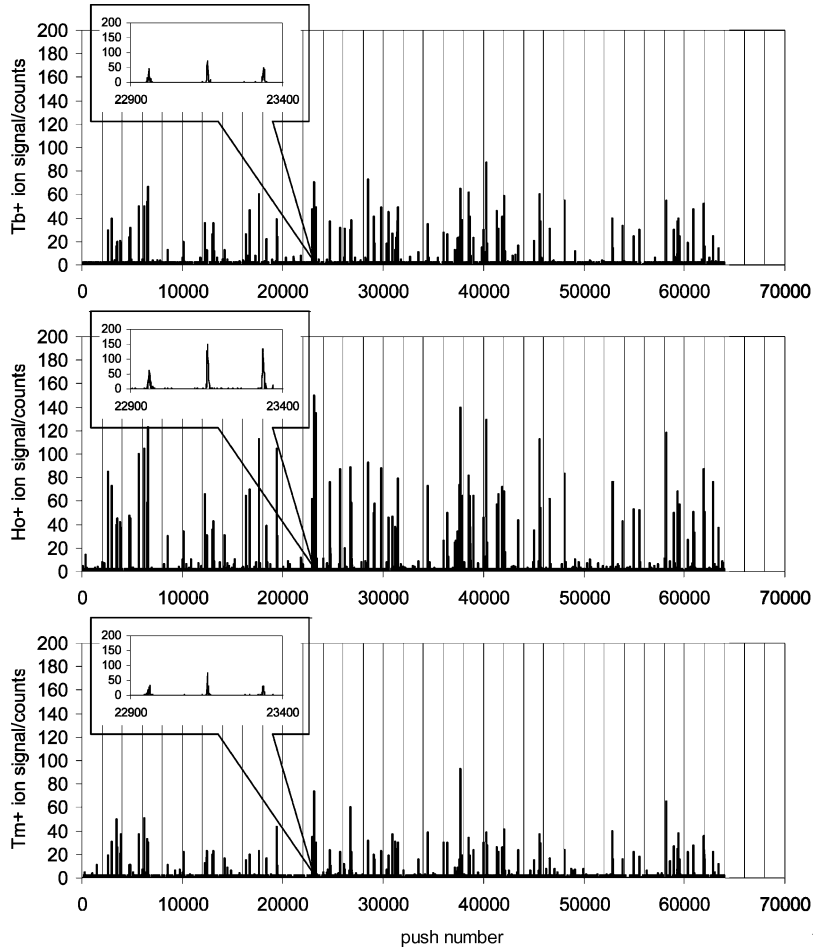

Figure 5. Dual counts signals for the first 64 000 spectra (0.83 s) of a 120 s continuous acquisition for a sample containing 2×10^6 beads/mL aspirated at 100 μL/min, each bead containing Tb, Ho, and Tm at 1:2:1 concentration.

At an introduction rate of 100 μL per min and concentration of ~2000 beads per μL, 400 000 beads were aspirated by the nebulizer in 120 s, of which 9 200 were detected. Thus the minimum transmission of the cyclonic spray chamber for these particles is 2.3%.

The instrument sensitivity at high resolution, measured in tuning mode, is 150 000 cps per ng/mL of Ho. A separate measurement with the spray chamber drain output cycled back to the sample container was done to assess the sample transport rate into the torch in tuning mode (~60 μL per min if evaporative loss is neglected), suggesting that the instrument transmission is 1 count per 2.5×10^4 atoms of Ho introduced into the plasma. The mean signal for the "brightest" labeling metal was ~400 counts per bead, suggesting that approximately 10^7 atoms of Ho per bead were present. From TEM photographs (not shown), the surface area coverage of the particles was estimated to be between 10 and 20% or $(1.4-2.9) \times 10^7$ amine groups per particle. This indicates that the average DTPA conjugation efficiency is between 35 and 70%. We attribute the relatively large (~40% RSD) spread of detected counts per transient to nonmonodispersity of the beads (diameter CV of 4%, stated by the manufacturer) and the spread of DTPA conjugation efficiency. Other factors contributing to the RSD might include plasma turbulence and radial dispersion. We are currently working on development of protocols for reproducible element-encoding of polystyrene beads to be used for instrument calibration, as well as for a massively multiplexed bead array assay, which will be described in a separate paper.

In the case of cell analysis, a Rh- or Ir-DNA intercalator is used to indicate the appearance of a cell event.[7] In this case, the algorithm for detecting cell-induced transients from the per-spectrum data includes summation of the ^{191}Ir and ^{193}Ir responses and comparing the (smoothed) sum to a selected threshold. The efficiency of the aerosol-splitter based cell introduction system, estimated from the frequency of the iridium signal transients for a given sample introduction rate (typically 60 μL/min) and the cell concentration in the samples (typically 1 million cells/mL), is currently 6−10%.

RESULTS AND DISCUSSION

Application to Multiplex Antigen Detection in Single Cells. The simultaneous determination of many antigens in a single cell has significant prognostic and diagnostic value. In the case of acute leukemias, distinction between lymphoid and myeloid types is of critical importance for correct therapy. In this application, subclassification of immunophenotypic features within these types by the CyTOF multiparameter analytical technique is capable of providing quantitative data on the expression of 20 or more biomarkers in parallel, thus positioning mass cytometry for use in personalized diagnosis and treatment. We present results obtained from single cell analysis of human leukemia cell lines and acute myeloid leukemia (AML) patient samples stained with 20 different metal-

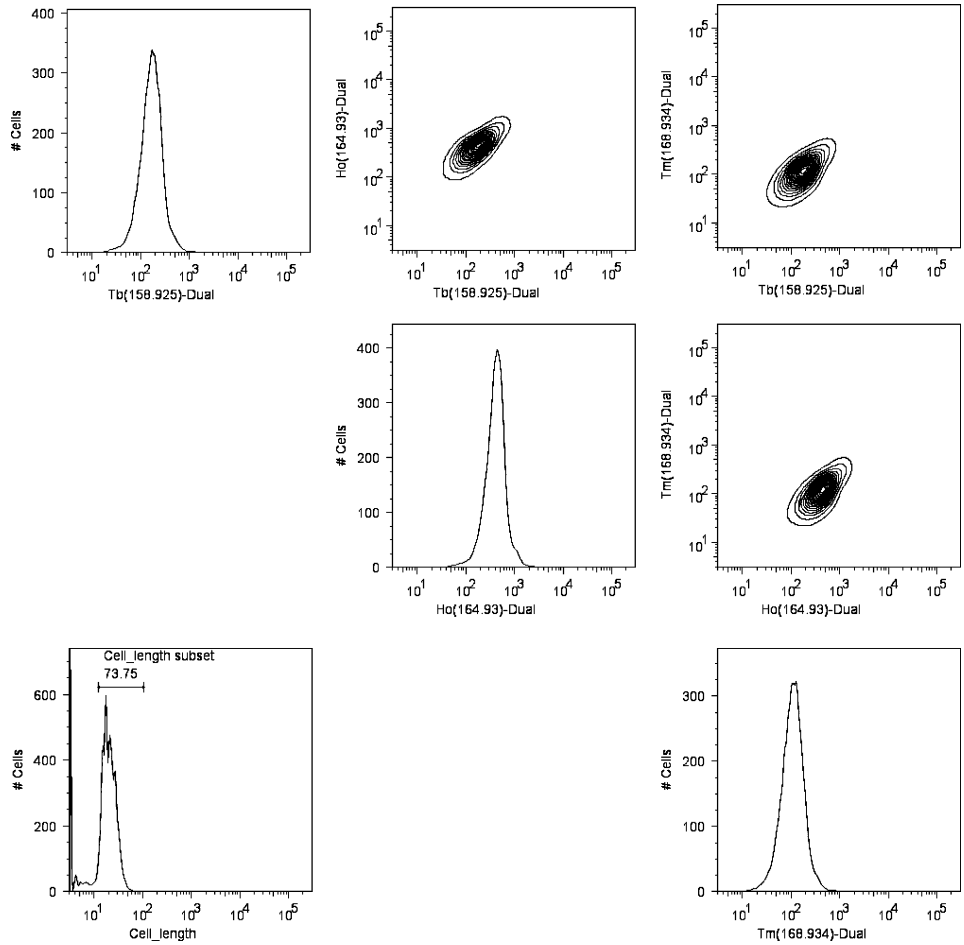

Figure 6. "Cell length" histogram for all above-threshold events (12 463), ion signal 2D 10% density contours, and ion signal histograms for 9 192 bead-induced transient events detected in 120 s measurements of Tb, Ho, and Tm-containing beads.

tagged antibodies. The immature myeloid (KG1a; *ATCC* CCL246.1) and B-lymphoblastoid (Ramos; ATCC CRL-1596) cell lines were grown under standard tissue culture conditions. Five frozen samples of mononuclear cells from blood or bone marrow corresponding to acute monoblastic/monocytic leukemia subtypes were a generous gift of the Quebec Leukemia Cell Bank.[34] The frozen samples were rapidly thawed in a 37 °C water bath and immediately diluted in medium with 40% FCS, prewarmed to 37 °C. Cell viability and numbers were obtained from the Vi-Cell (Beckman Coulter Inc., Fullerton, CA) automated cell counter. All samples were at least 82% viable (Trypan Blue-excluding cells). The cells were centrifuged and incubated for 60 min in cell growth media at 37 °C for metabolic recovery. A panel of 20 antibodies (BD Biosciences, San Jose, CA) selected against myeloid (CD13, CD14, CD15, CD33) and lymphoid (CD3, CD4, CD5, CD19, CD20, CD28, CD57) markers; nonlineage (CD34, CD38, CD117, HLA-DR) and differentiation markers (CD36, CD56, CD64, CD45, CD45RA) were labeled with MAXPAR element tags (DVS Sciences Inc., Richmond Hill, Canada). Antibody labeling has been described in detail elsewhere.[20] The list of antibodies and corresponding lanthanide isotopes is shown in Table 2.

A master mix of all element-tagged antibodies (0.5−2 ng/mL of each antibody) was prepared in 0.5% FBS/PBS and added to the cells. Washed cells were fixed (2% formaldehyde) and incubated with the Ir-intercalator for DNA staining.[35] Following several washes, the pelleted cells were resuspended in a low salt buffer at 10^6 cells/mL and analyzed on the mass cytometer. Data in FCS 3.0 format were used for cell population analysis with FlowJo software. Results are presented in Figures 7 and 8 as polar diagrams of median intensity values (logarithmic scale) for each antigen averaged over uniform cell populations (homogeneous cell lines and over 90% blast cells in the AML patient

Table 2. List of Antibodies against Surface Markers Tagged with Different Stable Isotopes[a]

surface markers	tag isotopes	surface markers	tag isotopes
CD15	^{139}La	CD45	^{159}Tb
CD33	^{141}Pr	CD5	^{164}Dy
CD4	^{142}Nd	CD38	^{165}Ho
CD13	^{144}Nd	CD36	^{166}Er
CD14	^{145}Nd	CD57	^{170}Er
CD117	^{146}Nd	CD34	^{169}Tm
HLA-DR	^{147}Sm	CD19	^{171}Yb
CD3	^{152}Sm	CD56	^{174}Yb
CD45RA	^{151}Eu	CD28	^{176}Yb
CD64	^{153}Eu	CR	^{127}I-contrast reagent
CD20	^{156}Gd	Ir	^{191,193}Ir-intercalator

[a] CR refers to iodine-containing contrast agent administered to patients; Ir refers to iridium-containing DNA intercalator.

(34) Quebec Leukemia Cell Bank, program funded by the cancer network of the Fonds de la Recherche en Santé du Québec (Réseau-Cancer FRSQ), http://www.bclq.gouv.qc.ca.

(35) Ornatsky, O. I.; Lou, X.; Nitz, M.; Schäfer, S.; Sheldrick, W. S.; Baranov, V. I.; Bandura, D. R.; Tanner, S. D. *Anal. Chem.* **2008**, *80*, 2539–2547.

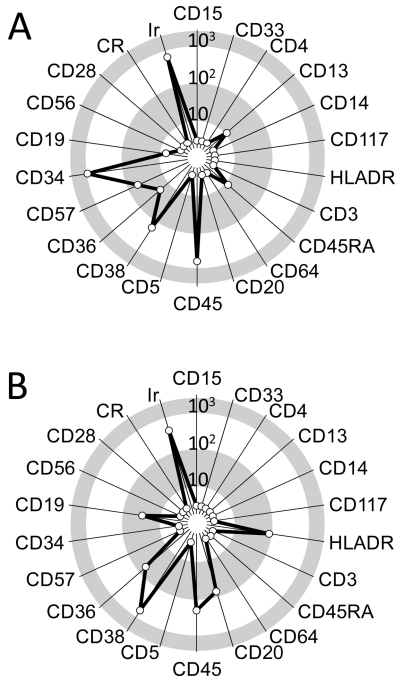

Figure 7. Polar diagrams of median intensity values for surface antigens measured using metal-tagged antibodies on model cell lines KG1a (A) and Ramos (B). Data collected on the mass cytometer and processed with FlowJo software. The typical population size used for averaging was 15 000−20 000 cells. Each of the 22 axes represents an antibody (or contrast reagent, CR, or Ir-DNA intercalator) measured by detecting the isotopic tags indicated in Table 2 per individual cell event.

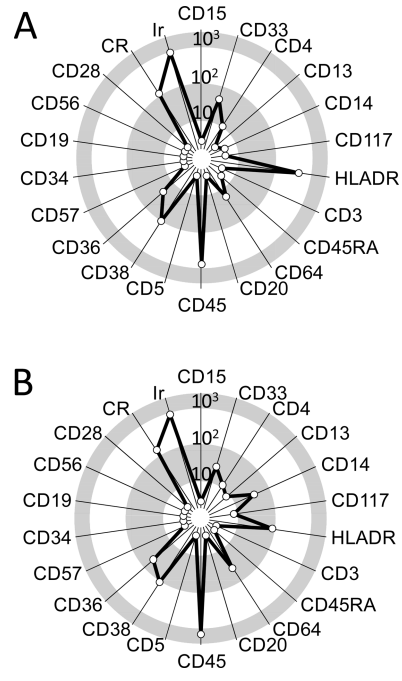

Figure 8. Polar diagrams of median intensity values for surface antigens measured using metal-tagged antibodies on leukemia patient samples, monoblastic M5 AML(A) and monocytic M5 AML (B). The monoblastic phenotype (A) shows high CD33 and HLA-DR and low CD34, CD13, CD14, and CD64 expression levels. The more differentiated monocytic M5 (B) type displays increased CD13, CD14, and CD64 and lower HLA-DR levels. Data were collected on the mass cytometer and processed with FlowJo software. The typical population size used for averaging was 15 000−20 000 cells. Each of the 22 axes represents an antibody (or contrast reagent, CR, or Ir-DNA intercalator) measured by detecting the isotopic tags indicated in Table 2 per individual cell event.

samples). KG1a cells (Figure 7A) display an immune phenotype very similar to that of primitive hematopoietic stem cells: high CD34, low HLA-DR, low CD33, absence of lymphoid markers,[36] whereas Ramos cells (Figure 7B) are considered representative of immature B-cells expressing high levels of lymphoid markers CD20, CD19 and high HLA-DR.[37] It is clear that the metal-tagged antibodies recognize respective antigens on the model cell lines when added simultaneously in a mixture. Of the five AML samples, three were classified as monoblastic and two as monocytic by two-color flow cytometry at the leukemia bank. The mass cytometry analysis confirmed that these groups were distinctly different from each other in respect to the expression of the 20 antigens and displayed immunophenotypes representative of monoblastic (Figure 8A) or monocytic (Figure 8B) AML. Similar to flow cytometric data received from the bank and published results,[38] the monoblastic phenotype (A) had high CD33 and HLA-DR and low CD34, CD13, CD14, and CD64 levels, while the more differentiated monocytic phenotype (B) displayed increased CD13, CD14, and CD64 and lower HLA-DR levels. Both groups were negative for CD34, CD19, and CD20, for example. Notice that the common leukocyte antigen CD45 was highly expressed by all cell types. An interesting feature of the AML samples was the detection of iodine (^{127}I), which could have been accumulated by the cells during diagnostic administration of an iodine-containing contrast reagent. Thus, the studied cell lines and subtypes of AML had distinct immunotypes identified by 20 parameter mass cytometry of single cells.

CONCLUSIONS

We have described a novel cytometric technology for the simultaneous immuno-detection of multiple antigens in single cells, which overcomes existing flow cytometry limitations resulting from fluorescent tag emission spectral overlap by utilizing multiple-atom elemental antibody tagging and a fast elemental reader based on a high sensitivity, high spectral rate inductively coupled-plasma time-of-flight mass spectrometer.

The application of the new technology to the simultaneous detection of 20 surface antigens in single cells of leukemia cell lines and leukemia patient samples is demonstrated. Element tagging coupled with elemental analysis of individual cells or beads provides new perspectives using polyparameter elemental signatures for cell characterization, elemental cell encoding, or in element-coded bead-based gene/protein arrays. The main advantages of the technology are practically no overlaps between detection channels, elemental response that is independent of the sample matrix resulting in the capability for absolute quantification, and simplified measurement protocol due to the stability of elemental tags.

Since particles are completely disintegrated during the analysis, the technology does not provide cell sorting capability. Although

(36) Clave, E.; Carosella, E. D.; Gluckman, E.; Dubray, B.; Socie, G. *Int. J. Radiat. Oncol. Biol. Phys.* **1996**, *35*, 709–719.
(37) Rousset, F.; Malefijt, R. D.; Slierendregt, B.; Aubry, J. P.; Bonnefoy, J. Y.; Defrance, T.; Banchereau, J.; Devries, J. E. *J. Immunol.* **1988**, *140*, 2625–2632.
(38) Tallman, M. S.; Kim, H. T.; Paietta, E.; Bennett, J. M.; Dewald, G.; Cassileth, P. A.; Wiernik, P. H.; Rowe, J. M. *J. Clin. Oncol.* **2004**, *22*, 1276–1286.

this may be perceived as a disadvantage, for analytical purposes it relieves the need to retag and remeasure cells, since an all-antigens panel cell characterization is done during a single measurement. The highest theoretical cell analysis throughput, approximately 3 000 cells per second, is physically limited by the need to separate ion clouds produced in the plasma ion source for separate cells (the event duration for which is the time required for a given ion plume derived from a single cell to pass the sampling aperture, e.g., a 2 mm diameter plume flowing at 10 m/s yields a 200 μs duration event). Our present efforts are focused on improving the cell transport efficiency through the cell introduction system. Further refinements of the data collection and processing algorithms (either by dedicated signal processing in the signal digitizer or parallel processing during the next sample data collection) will make it possible to obtain per-cell results online. Another significant focus of technology development is related to the representation of more than 20-dimensional data. For the methodology to be useful in delivering a "yes−no" answer in rare cell identification and disease diagnostics, we are developing multiparameter clustering algorithms with a self-training neural network.

An additional benefit of using a TOF mass analyzer for individual cell analysis is that unasked questions might be answered by the elemental data. For example, the "treatment history" of the sample might be revealed by the presence of iodine or barium used as imaging contrast agents (as shown above), heavy (m > 100 Da) radioisotopes from immuno-radiotherapy, cisplatin, or colloidal-gold treatments. Further, insight into treatment efficiency with metalo-drugs such as cisplatin might be obtained by relating the antigen signature of a cell to the abundance of drug-derived elements in the cell. We believe that the availability of a convenient and reliable means to quantitatively determine many (N > 10) orthogonal disease/rare cell markers in individual cells will change the questions that biologists ask and may transform the current methods of investigating cell genesis and disease detection.

ACKNOWLEDGMENT

This project was funded by Genome Canada through the Ontario Genomics Institute, the Ontario Institute for Cancer Research, the Ministry of Research and Innovation of Ontario, and by DVS Sciences Inc. Provision of the Ir intercalator by S. Schäfer and W. S. Sheldrick of Ruhr-Universität Bochum (Germany) is greatly appreciated. Provision of leukemia patient samples by the Quebec Leukemia Cell Bank (BCLQ) is gratefully acknowledged. The in-kind contributions of detectors by ETP and vacuum pumps by Oerlikon Leybold are appreciated.

Received for review May 14, 2009. Accepted July 1, 2009.

AC901049W